Er^{3+}doped Bismuth oxide tertiary glass as a temperature sensing probe

Garima Tripathi, S.B. Rai *
Laser and Spectroscopy Laboratory, Department of Physics,
Banaras Hindu University, Varanasi 221005, India

Abstract

Radiative properties of Er^{3+}-doped tertiary bismuth glass has been analyzed by the Judd–Ofelt theory. NIR to visible upconversion in the Er^{3+}-doped glass has been reported. The mechanism for the upconversion is explained on the basis of quadratic dependence on excitation power and on the energy-matching scheme. Energy transfer is noted as the dominant process including the long-lived $^4I_{11/2}$ level as the intermediate state for the green and red upconversion emissions.
It is found that the fluorescence intensity of the rare earth ion in the glass strongly depends on the glass temperature

$$I = I_0 e^{-E/kT}$$

Thus, the fluorescence intensity emitted by an ion can be used to estimate the temperature. The effect of temperature on the fluorescence intensity of the two bands due to $^2H_{11/2} \rightarrow {}^4I_{15/2}$ and $^4S_{3/2} \rightarrow {}^4I_{15/2}$ transitions as well as on the transitions due to Stark components of the $^4S_{3/2}$ level have been monitored and it is concluded that their intensity ratio may serve as better temperature sensing device.

1. Introduction

Compared to conservative temperature monitoring devices, optical based systems are particularly advantageous for operation in electromagnetically and thermally harsh environments, enabling temperature control of industrial processes at electrical power stations, in buildings and also for fire detection [1]. Er^{3+}doped glasses have also been used as temperature sensors because of its favorable energy level structure. There has been great activity in recent years to investigate the upconversion of near infrared and visible radiation into visible/UV light because of applications in, display devices, optical data storage, biomedical diagnostics, sensors, optical fiber and under sea optical communications [2, 3]. Other rare earth ions like Pr^{3+}, Dy^{3+}, Ho^{3+}, Eu^{3+}, Tm^{3+} have also been extensively studied for the upconversion process in various kinds of crystals / glasses [4-15]. The oxide glasses having small absorption coefficient within the wavelength range of upconversion emission and with high chemical and thermal durability, are considered suitable materials for technological applications.

However, the high phonon energy corresponding to the stretching vibrations of the oxide glass network is generally a constraint in efficient upconversion. Bismuth oxide glass is a high refractive index and low phonon energy system and upconversion luminescence (Er^{3+}) has been observed in this host [16, 17]. Optical properties of GeO_2-PbO-Bi_2O_3 and GeO_2-

Bi_2O_3 systems have been studied in the past and these were found as good candidates for applications as host in non linear optics, optical amplification and upconversion fiber optical devices [18]. According to Chen et al [19] PBB (PbO-Bi_2O_3-B_2O_3) glass has best water endurance.

In this chapter we report the optical properties of Er^{3+} doped barium lead bismuth oxide glass. This glass includes oxides of heavy metals such as lead, barium and bismuth and is expected to have excellent spectral properties. The density, refractive index and other physical properties of this tertiary glass were measured. Optical absorption and emission spectra were investigated. Optical emission probabilities for each transition have been studied through J-O theory. The visible emission has been also observed under 800nm excitation and the upconversion mechanism has been discussed. The effect of temperature on the upconversion luminescence intensity of the two lines (coming from the two close lying thermally coupled levels $^2H_{11/2}$ and $^4S_{3/2}$ to a common lower level $^4I_{15/2}$) as well as on the Stark components ($^4S_{3/2}(1) \rightarrow {}^4I_{15/2}$ and $^4S_{3/2}(2) \rightarrow {}^4I_{15/2}$) of the $^4S_{3/2} \rightarrow {}^4I_{15/2}$ transition have been monitored and it is noted that the two Stark components of this transition may also be used to estimate the temperature over a wide range with appreciable sensitivity.

2. Experimental details

The doped glasses utilized in the present study were synthesized by quenching method. The molar composition of the glass was as follows

$$(60\text{-}x)\ Bi_2O_3 + 20\ Li_2CO_3 + 10\ BaCO_3 + 10\ PbO + x\ Er_2O_3 \qquad (1)$$

where x = 0.1, 0.25, 0.5, 1.0, 1.25 and 1.5 mol%

The well-mixed raw material (5gm) was melted at 950^0C for 30 min in a platinum crucible. The molten mass was then poured into a stainless steel cast. The transition temperature of the glass is ~500^0C. The molten mass was annealed at a temperature of~400^0C to minimize strain and then allowed to cool slowly to room temperature. The glass thus obtained was polished carefully in order to meet the optical requirements. Care was taken to avoid moisture during the preparation of the glass. Infrared absorption measurements were made with a Perkin Elmer FTIR spectrometer. The density and the refractive index of the sample was measured using Archimedes principle (using Xylene as an immersion liquid) and Brewster's angle polarization method (using 632.8 nm radiation from a He-Ne laser).

The value of the density and the refractive index for the present glass with 1.0 mol% of $Er^{3+}$are 7.61g/cm^3 and 2.25 respectively.

The fluorescence spectra of the glasses with different concentrations of Er^{3+} were excited using 532nm line of $NdYVO_4$ laser. It was observed that fluorescence yield is maximum for 1.0mol% concentration of Er^{3+}. Therefore, the glass with this concentration was used in further studies. The upconversion spectrum was recorded for this glass using 800 nm line from a Ti-sapphire laser. The fluorescence emitted by the doped glass was dispersed by a 0.5m monochromator attached with a S-20 photomultiplier tube. The absorption spectrum of the glass was recorded using a Varian Spectrophotometer.

For the temperature measurements the doped glass was placed in a small furnace (attached with a thermometer) with holes in two perpendicular directions for entrance and the exit of NIR laser and the fluorescence radiations.

3. Results and Discussion

3.1 Absorption Spectrum

Fig 1 shows the absorption spectrum of 1.0mol% Er^{3+} doped in Bi_2O_3-Li_2O-BaO-PbO glass in the 400-1700 nm region. From the figure, it is clear that there are seven peaks at 1532, 976, 800, 653, 547, 521 & 488 nm in the spectrum corresponding to absorption from the ground state $^4I_{15/2}$ to the excited states $^4I_{13/2,}$ $^4I_{11/2}$ $^4I_{9/2}$, $^4F_{9/2}$, $^4S_{3/2}$, $^2H_{11/2}$ and $^4F_{7/2}$ respectively.

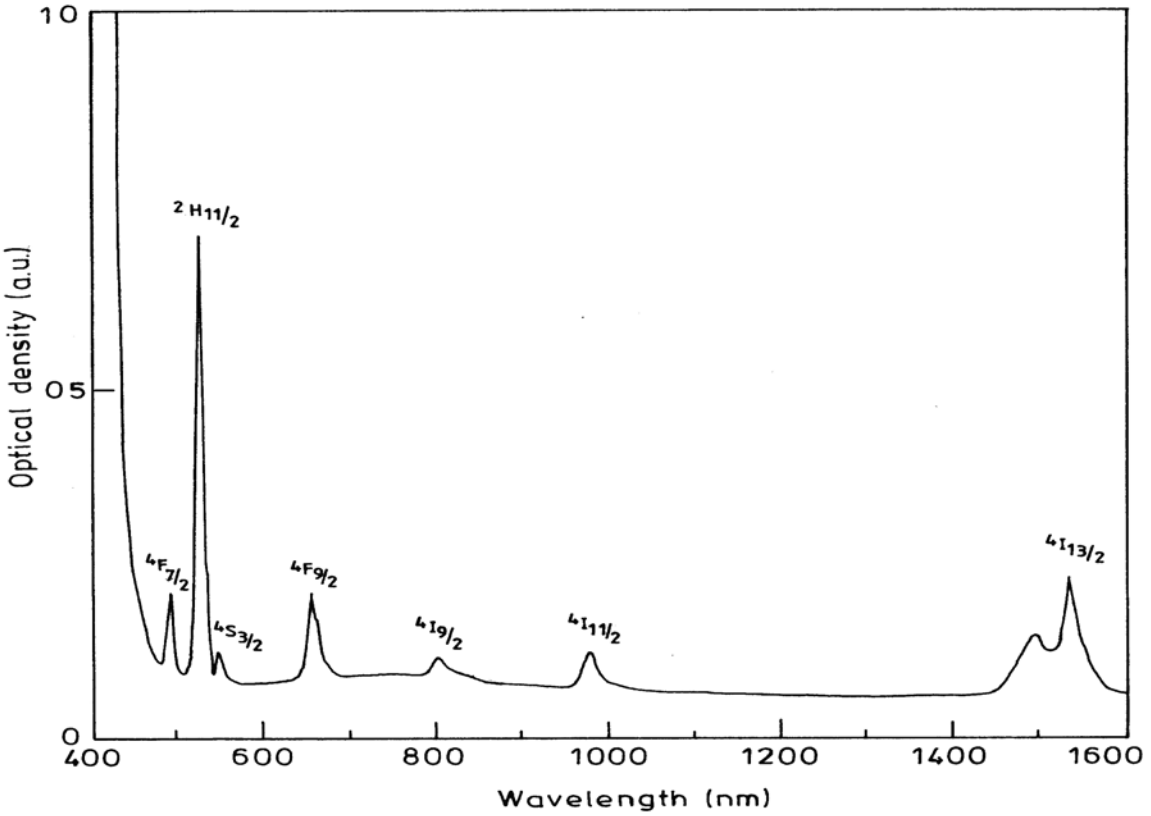

Fig 1 Absorption spectra of 1 mol% Er^{3+} doped BiLiBaPb tertiary glass

The oscillator strengths for the different transitions have been calculated and the values obtained for different transitions are given in Table 1.

Table 1. Measured and calculated oscillator strength of Er^{3+}(1 mol%) doped in BiLiBaPb glass

Transition	f_{exp}	f_{cal}
$^4I_{15/2}\rightarrow{}^4I_{13/2}$	3.33	3.15
$^4I_{15/2}\rightarrow{}^4I_{11/2}$	0.66	1.61
$^4I_{15/2}\rightarrow{}^4I_{9/2}$	0.16	0.21
$^4I_{15/2}\rightarrow{}^4F_{9/2}$	3.24	2.87

$^4I_{15/2} \rightarrow {}^4S_{3/2}$	-	1.27
$^4I_{15/2} \rightarrow {}^2H_{11/2}$	16.89	16.91
$^4I_{15/2} \rightarrow {}^4F_{7/2}$	4.21	4.28

Table 2. Electric dipole line strength, Radiative transition probabilities, branching ratio and radiative lifetime for excited levels of Er^{3+}: BiLiBaPb glass**.**

SLJ	S'L'J'	Energy (cm^{-1})	S'ed ($x10^{-22}$)	A_{ed} (s^{-1})	β_R	τ (ms)
$^4I_{9/2}$	$^4I_{11/2}$	2295.7	30.61	3.3455	.0064	
	$^4I_{13/2}$	6604.6	136.44	354.884	.6833	0.2328[20]
	$^4I_{15/2}$	12500	9.14	161.1476	.3102	
				ΣA= 519.3751		1.925
$^4F_{9/2}$	$^4I_{9/2}$	2824.4	91.79	18.67	.0046	0.0623[20]
	$^4I_{11/2}$	5120.1	289.99	351.356	.0858	
	$^4I_{13/2}$	8889	28.75	182.264	.0445	
	$^4I_{15/2}$	15314	109.31	3543.679	.8652	0.244
				ΣA=4095.97		
$^4S_{3/2}$	$^4F_{9/2}$	3130.5	4.844	3.35	0.0004	1.06[20]
	$^4I_{9/2}$	5955.9	50.862	242.52	0.0278	
	$^4I_{11/2}$	8251.6	14.897	188.92	0.0217	
	$^4I_{13/2}$	12021	64.599	2532.42	0.2911	
	$^4I_{15/2}$	18282	41.566	5731.98	0.6589	
				ΣA= 8699.18		0.115
$^2H_{11/2}$	$^4I_{15/2}$	19011	524.21	27094.99		.0369
$^4F_{7/2}$	$^2H_{11/2}$	1404.2	166.86	5.211	0.0004	
	$^4S_{3/2}$	2159	.2997	0.032	…….	
	$^4F_{9/2}$	5289	11.9501	19.950	0.0016	
	$^4I_{11/2}$	8114	42.562	256.643	0.0205	
	$^4I_{13/2}$	10401	14.3092	181.676	0.0145	
	$^4I_{15/2}$	20490	123.9706	12033.77	0.9629	
				ΣA= 12497.29		0.08

These values have been used to calculate the Judd-Ofelt intensity parameters. The intensity parameters thus obtained have been used to determine various optical properties such as electric dipole line strength, transition probability, radiative lifetime, branching ratio etc. (see Table 2.).

The oscillator strength (f) of the absorption bands are determined experimentally using the relation

$$f_{\text{exp.}} = 4.32\times10^{-9}\int \varepsilon(\nu)d\nu \qquad (2)$$

where $\varepsilon(\nu)$ is the molar extinction coefficient at energy ν cm^{-1}.

The J-O theory [21,22] gives the oscillator strength f of a transition from the ground state to an excited state for an electric dipole transitions as

$$f_{cal.} = \left[\frac{8\pi^2 mc\,\nu}{3h(2J+1)}\right]\frac{(n^2+2)^2}{9n}\sum_{\lambda=2,4,6}\Omega_\lambda\left|\left(\psi_J\left\|U^\lambda\right\|\psi_{J'}\right)\right|^2 \qquad (3)$$

where 'ν' is the energy of transition in cm^{-1}, U^λ (λ=2,4,6) are unit tensor operators of rank λ and Ω_λ are the J-O intensity parameters. The terms $\left(\psi_J\left\|U^\lambda\right\|\psi_{J'}\right)$ are the reduced matrix elements. These matrix elements for a majority of rare earth ions are not very sensitive to crystal field surrounding the lanthanide ion [19].

Eqn. (2) allows us to determine the oscillator strength $f_{\text{exp.}}$ for different transitions and these values have been used in eqn. (3) to determine the J-O intensity parameters. The spontaneous radiative transition probability between J and J' levels for electric dipole transitions is given by

$$A_{JJ'} = \frac{64\pi^4\nu^3}{3h(2J+1)}\frac{n(n^2+2)}{9}e^2\sum_{\lambda=2,4,6}\Omega_\lambda\left|\psi_J\left\|U^\lambda\right\|^2\psi_{J'}\right|^2 \qquad (4)$$

The radiative lifetime of an excited state is calculated by $\tau_R = \left(\sum_{J'} A_{JJ'}\right)^{-1}$ (5)

and the branching ratio $\beta_{JJ'}$ corresponding to the emission from level J to J' is given by

$$\beta_{JJ'} = A_{JJ'}\tau_R \qquad (6)$$

stimulated emisson cross section is given by the relation

$$\sigma = \frac{\lambda^4}{8\pi^2 cn^2\Delta\lambda}A(\psi'_{J'} \rightarrow \psi_J) \qquad (7)$$

3.2 Upconversion Spectra

The upconverted luminescence spectrum of 1.0mol% Er^{3+} doped glass under excitation with ~800 nm NIR radiation is shown in Fig 2. Intense green emission bands around 513-538 and 538-547 nm are observed.

These bands are due to $^2H_{11/2}\rightarrow {}^4I_{15/2}$ and $^4S_{3/2}\rightarrow {}^4I_{15/2}$ transitions. Along with this a weak band is also observed at 654 nm due to the $^4F_{9/2}\rightarrow {}^4I_{15/2}$ transition. $^2H_{11/2}\rightarrow {}^4I_{15/2}$ and $^4S_{3/2}\rightarrow {}^4I_{15/2}$ transitions each are found to consist of two components at 526, 535 nm and at 547, 556 nm respectively. No blue emission around 400nm was detected from Er^{3+} in this lattice. This

may be attributed to the low incident laser intensity used in our experiments, since this blue emission generally involves a three step excitation. It is observed that the energy separation between $^2H_{11/2}$ and $^4S_{3/2}$ states is around 730 cm^{-1} for the present glass. Thus even at room temperature thermalization for the two levels can occur.

The upconversion intensity I_{up} is proportional to the n^{th} power of the NIR excitation intensity (I_{NIR}) i.e I_{up} α $(I_{NIR})^n$, where n is the number of NIR photons absorbed in emission of a single visible photon. Thus a plot of log I_{up} versus log I_{NIR} would yield a straight line the slope of which would define the number n of photons absorbed. Fig 3 shows such a plot for $^2H_{11/2}\rightarrow {}^4I_{15/2}$, $^4S_{3/2}\rightarrow {}^4I_{15/2}$ and $^4F_{9/2}\rightarrow {}^4I_{15/2}$ transitions and the slopes corresponding to the three transitions are 1.91, 1.80 and 1.63 respectively. This indicates that two incident photons are involved in populating the three levels viz $^2H_{11/2}$, $^4S_{3/2}$ and $^4F_{9/2}$ levels.

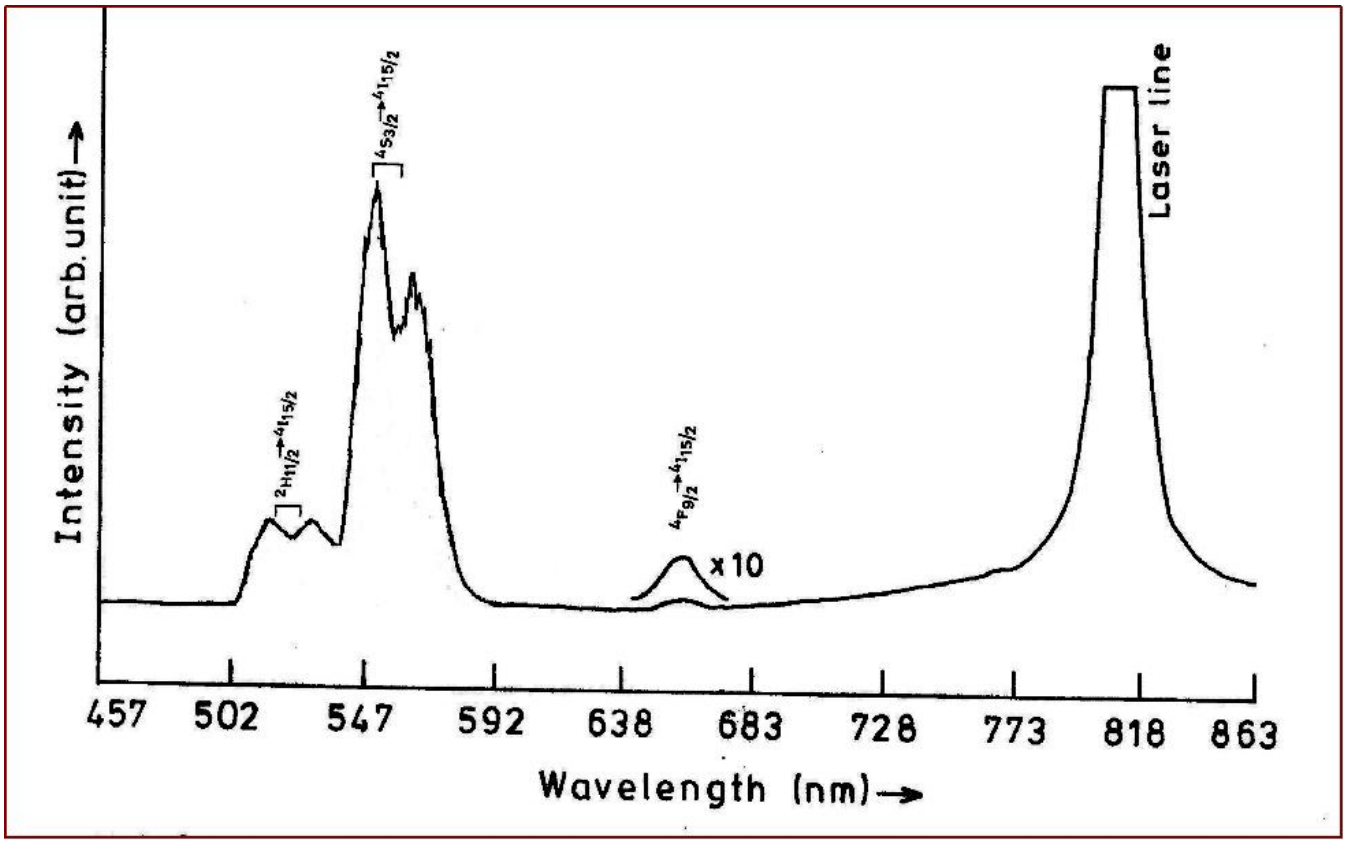

Fig 2 Upconversion Fluorescence spectrum 1.0 mol% Er^{3+} BiLiBaPb tertiary glass under 800 nm excitation

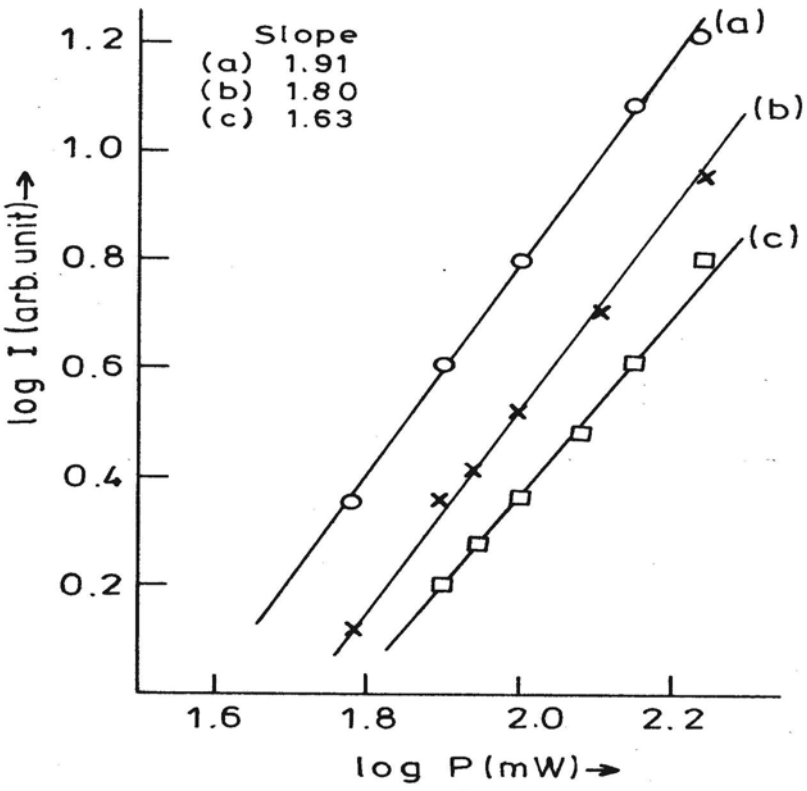

Fig 3 Dependence of upconversion fluorescence intensity on excitation power under 800nm excitation corresponding to the (a) $^2H_{11/2}\rightarrow$ $^4I_{15/2;}$ (b) $^4S_{3/2}\rightarrow ^4I_{15/2;}$ and (c) $^4F_{9/2}\rightarrow$ $^4I_{15/2}$ transitions

The upconversions may be either due to two photon absorption through excited state absorption (ESA) or through energy transfer (ET). The upconversions are seen even at very low power of the incident laser. Therefore, upconversion emission by two photon absorption is ruled out. In ESA, ions in a state excited by the absorption of an incident photon absorb another photon having the same energy to go to a still higher excited state. The excited ions then decay to the ground state or to an intermediate excited state emitting photons with energy higher than the incident photon energy.

In case of energy transfer (ET) process, an excited ion in the intermediate state transfers its excitation energy to another near by excited ion; Thus the donor ion itself comes to the ground state and the other ion which receives this additional energy is promoted to the higher energy state. The upconversion by this process would strongly depend on the concentration of the rare earth ions. We measured the upconversion spectrum for glasses with different concentrations of Er^{3+}. It was observed that weak green upconversion appears even at 0.1mol% Er^{3+} in the glass. Therefore ESA is the most probable channel which contributes to the upconversion process. The intensity of the upconversion bands increases rapidly with an increase of Er^{3+} concentration, so it appears that energy transfer also plays a role and at higher concentrations energy transfer plays a more dominant role. The mechanism for the upconversion is depicted in Fig 4. Initially, the Er^{3+} ions are

excited to $^4I_{9/2}$ state on excitation with 800 nm laser light. The ions in $^4I_{9/2}$ level relax to the $^4I_{11/2}$ level (as the lifetime of $^4I_{9/2}$ level is much smaller than that of $^4I_{11/2}$ level). The ions in $^4I_{11/2}$ level absorb another incident photon (800nm) and are promoted to high lying excited state. These ions after relaxation populate the $^2H_{11/2}$ and $^4S_{3/2}$ states which are responsible for the green fluorescence.

At higher concentrations an ion in the $^4I_{11/2}$ state transfers its excitation energy to a neighboring excited ($^4I_{11/2}$) Er^{3+} ion and itself returns to the ground state whereas the second ion moves upward to the $^4F_{7/2}$ state. The ions in the $^4F_{7/2}$ state relax nonradiatively to $^2H_{11/2}$ and $^4S_{3/2}$ levels which are the upper states for the transitions giving visible photons in the green region. The mechanism may be expressed as:

$$^4I_{11/2}\,(Er^{3+}) + {}^4I_{11/2}\,(Er^{3+}) \rightarrow {}^4F_{7/2}\,(Er^{3+}) + {}^4I_{15/2}\,(Er^{3+}) \qquad (8)$$

$$^4F_{7/2}\,(Er^{3+}) \rightarrow {}^4S_{3/2,}\,{}^2H_{11/2}\,(Er^{3+}) + \Delta E \qquad (9)$$

$$^4S_{3/2,}\,{}^2H_{11/2}\,(Er^{3+}) \rightarrow {}^4I_{15/2}\,(Er^{3+}) + h\upsilon \qquad (10)$$

Some of the excited Er^{3+} ions in $^4S_{3/2}$ and $^2H_{11/2}$ relax nonradiatively to $^4F_{9/2}$ level also. This gives red fluorescence due to $^4F_{9/2} \rightarrow {}^4I_{15/2}$ transition. Another possible channel for populating $^4F_{9/2}$ level may be that some of the ions present in the $^4I_{11/2}$ state relax non-radiatively to the $^4I_{13/2}$ level also.

Two ions in $^4I_{11/2}$ and $^4I_{13/2}$ levels may share their excitation energies to populate the $^4F_{9/2}$ level directly.

$$^4I_{11/2} + {}^4I_{13/2} \rightarrow {}^4F_{9/2} \qquad (11)$$

Another possible channel may be that

$$^4I_{13/2} + {}^4S_{3/2} \rightarrow 2\,{}^4F_{9/2} \qquad (12)$$

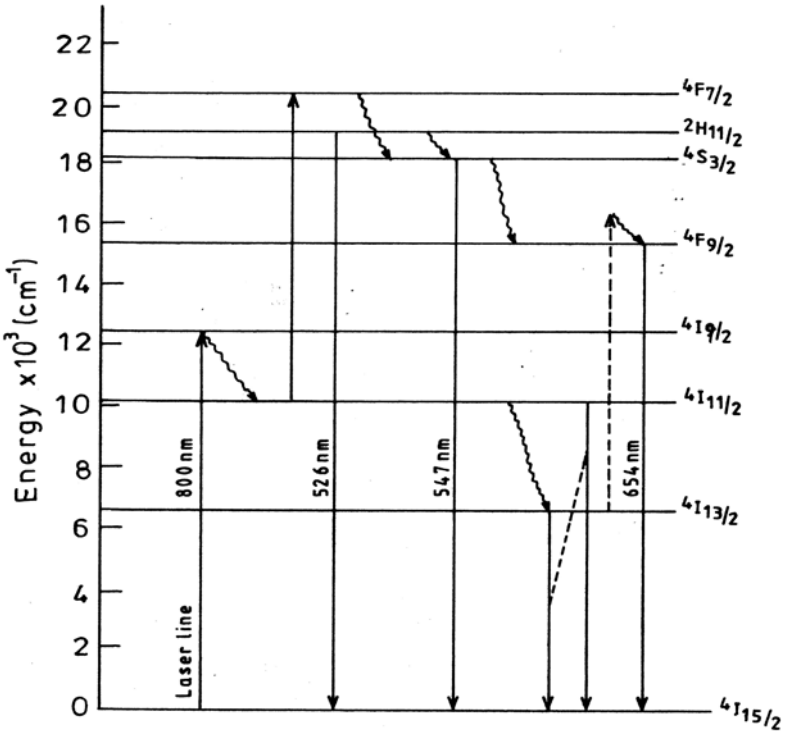

Fig 4 Energy level diagram of Er^{3+}

3.3Effect of temperature in the upconversion luminescence:

Determination of temperature of the source

It is found that the intensity of fluorescence from a rare earth ion in glass strongly depends on the glass temperature.

$$I = I_0 e^{-\Delta E / KT} \qquad (13)$$

Thus, the fluorescence intensity emitted by an ion can be used to estimate the temperature. This estimation however is vitiated due to fluctuations in the excitation power and environmental changes. These problems can be avoided if instead of one level one compares the fluorescence intensity emitted at different temperatures by ions in two close lying levels thermally coupled to each other. The ratio of the intensities of the fluorescence from two closed lying energy levels i.e. FIR [23, 24] may be expressed as,

$$\text{FIR} = I_2/I_1 = \frac{g_2 \sigma_{20} w_{20}}{g_1 \sigma_{10} w_{10}} e^{-\frac{\Delta E}{kT}} = Be^{-\Delta E/kT} \qquad (14)$$

where $B = \frac{g_2 \sigma_{20} w_{20}}{g_1 \sigma_{10} w_{10}}$

In this relation, I_i is the fluorescence intensities from the two (close lying levels) of the rare earth, σ_{ij} is the emission cross-section, g_i is the degeneracy of the level, w_{ij} is the transition frequency and ΔE is the energy separation between the two levels. Fluorescence intensity ratio method had been proposed for temperature sensing as early as in1976 Kusama et al [25].

We measured the fluorescence intensity for the two bands due to $^2H_{11/2} \rightarrow {}^4I_{15/2}$ and $^4S_{3/2} \rightarrow {}^4I_{15/2}$ transitions and, also for the two Stark components ($^4S_{3/2}(1) \rightarrow {}^4I_{15/2}$ and $^4S_{3/2}(2) \rightarrow {}^4I_{15/2}$) due to $^4S_{3/2} \rightarrow {}^4I_{15/2}$ transition at different temperatures.

The fluorescence intensities of the two bands viz. $^2H_{11/2} \rightarrow {}^4I_{15/2}$ and $^4S_{3/2} \rightarrow {}^4I_{15/2}$ have been measured in the 295-428K temperature range. As the two levels ($^2H_{11/2}$ and $^4S_{3/2}$) are close and thermally coupled to each other, other factors are not expected to much affect the measurements. Thus, if the intensities of the two bands at different temperatures are measured, their ratios can be used to determine the temperature as the intensity ratio of the two fluorescence peaks would depend on the thermal population distributions. The measured fluorescence intensity ratios of the two bands ($^2H_{11/2} \rightarrow {}^4I_{15/2}$ and $^4S_{3/2} \rightarrow {}^4I_{15/2}$) in the present case are given in Table 3. We have also put a thermo couple to measure the temperature. The temperatures read by the thermocouple are also listed.

Table 3. A comparison of the temperature determined by FIR of $^4S_{3/2} \rightarrow {}^4I_{15/2}$ and $^2H_{11/2} \rightarrow {}^4I_{15/2}$ transitions of Er^{3+} to that read by a thermocouple.

$I(^2H_{11/2} \rightarrow {}^4I_{15/2})/I(^4S_{3/2} \rightarrow {}^4I_{15/2})$	Temperatures calculated by FIR (K)	Temperatures observed by thermocouple (K)
0.244	292±0.60	295
0.378	330±0.03	328
0.470	355±0.25	358
0.610	388±0.02	388
0.741	419±0.05	428

The temperature of the doped glass as estimated by FIR show reasonable agreement with the one read by thermocouple. The larger deviation between the two values seen at higher temperatures is due to the large uncertainty in the measurement of the intensities as these are relatively small. The fact that the glass becomes softer at higher temperature may also be a contributing factor. The errors in the temperature are calculated using the relation $\Delta T = \frac{KT^2 \Delta FIR}{\Delta E.FIR}$ (15) and the values obtained are also given with the measured value in the same table.

As mentioned earlier the $^4S_{3/2}$ level shows two Stark components. It is also observed that the intensities of the two Stark components also changes in different ways with the change of temperature. We measured the intensity of the two components in between 295-600 K. The ratio of the intensities of the two components is given in Table 4**.** The separation between the two Stark sublevels is ~263 cm^{-1} i.e. they are thermally coupled with each other. It is seen that for higher

temperature of the glass the intensity of the two peaks becomes comparable though small. The intensity ratio of the two peaks are measured and used to estimate the temperature. The values thus obtained are compared with the values measured using the thermocouple in Table 4.

Table 4. Fluorescence intensity ratio (FIR) of the transitions of Stark components of $^4S_{3/2}$ level, temperature calculated by using FIR and measured using thermocouple

Fluorescence intensity ratio of the Stark components $[(^4S_{3/2}(1) \rightarrow {}^4I_{15/2})/ (^4S_{3/2}(2) \rightarrow {}^4I_{15/2})]$	Temperature calculated by FIR(K)	Temperature observed by thermocouple (K)
0.81	297±0.58	295
0.92	329±1.56	328
0.99	353±0.99	358
1.09	388±0.36	388
1.18	422±0.79	428
1.30	473±4.09	476
1.40	523±1.55	523
1.54	603±3.12	603

From Table 4 it is found that this ratio may serve as a more sensitive device upto 600K. Beyond this limit the glass become soft and therefore the measurements become difficult. Thus from the above studies it is concluded that not only the two different levels which are thermally coupled with each other but also the two Stark sublevels of a particular level having very small energy difference can be utilized to measure the temperature where normal conventional temperature sensors can not be used.

4. Conclusions

The spectroscopic properties of Er^{3+} doped in BiLiBaPb glass has been analyzed on the basis of J-O theory. Upconversions observed in Er^{3+} BiLiBaPb doped glass host are reported and explained. It is noted that the fluorescence intensity ratio (FIR) of the two thermally coupled close lying levels ($^2H_{11/2,}$ $^4S_{3/2}$) of Er^{3+} and for the two Stark sublevels of $^4S_{3/2}$ level can be used to measure temperature with appreciable sensitivity.

Acknowledgements

Authors are grateful to CSIR NewDelhi and DST,NewDelhi for financial assistance.

References

1. D.N. Messias,M.V.D.Vermelho,A.S.Gouveia Neto and J.S.Aitchison, Rev.Sci. Instru., 73(2002) 476.

2. G.A. Kumar, R. Riman, S. C. Chal, Y.N. Jang, I. K. Bal and H.S. Moon, J. Appl. Phys., 95 (2004) 243.
3. T. Sun, Z.Y. Zhang and K.T.V Grattan, Rev. Sci. Instrum.,71 (2000)4017.
4. E. Osiac, E. Heumann, G. Huber, S. Kuck, E. Sani A. Toncelli and M. Tonelli, Appl. Phys Lett, 82 (2003) 3832.
5. Vineet Kumar Rai, S. B. Rai and D.K. Rai, Opt. Comm., 257 (2006) 112.
6. J. Qiu, M. Shojiya, R. Kanno, Y. Kawamoto and M. Takahashi, J.Phys Condens Matt., 10 (1998) 11095.
7. F. Gan, J. Wang, and Y. Chen, J.Non.Cryst. Solids, 213&214 (1997)261.
8. F. Lanoz, I. R. Martin, J. M. Ramos and P. Nunez, J. Chem. Phys., 120 (2004) 6180.
9. S. Hode, S. Jiang, X. Peng, N. Peyghambarian, T. Luo and M. Morrell, Opt. Mat., 25 (2004) 149.
10. Y.Gao, Q. H. Nie, T. F. Xu and X. Shen, Spectrochim Acta A, 61 (2005)1259.
11. P. S. Peizel and A. Meijerink, Chem. Phys. Lett., 401 (2005) 241.
12. H. Lin, G. Meredith, S. Jiang, X. Peng, T. Luo, N. Peyghambarian and E.Y.B Pun. J. Appl. Phys., 93 (2006) 186.
13. N. Jaba, A. Kanoun, H. Mejri, A. Selmi, S. Alaya and H. Maare, J. Phys Condens. Matter, 12 (2004) 4523.
14. A. S. Oliveria, M.T. de.Araujo , A. S. Gouveia-Neto, A. S. B.Sombra, J.A. Medeiros Neto and N. Aranha, J. Appl.Phys., 83 (1998) 604.
15. M. Zambell, A. Speghini, G. Ingletto, C. Locatelli, M. Bettinelli, F. Vetrone, J.C. Boyer and J. Capabianco Opt. Mat., 25 (2004) 215.
16. S.Q.Man, E.Y.B.Pun and P.S. Chung, Appl. Phys. Lett, 77 (2000) 483.
17. H. Sun, S. Xu, L. Zhang, J. Wu, J.Zhang, L.Hu and Z. Jiang, Mat. Sci. Eng. A, 394 (2005) 83.
18. L.R.P.Kassab, A.de Oliveirs, W.Lozano, F.X.de.Sa and G.Macial, J.Non Cryst. Solids 351(2005) 3468.
19. Q. Chen ,M. Ferraris,Y.Menke,D.Milanese and E.Monchiero, J.Non.Cryst.solids, 324 (2003)1.
20. A. Florez, Y. Messaddeq, O. L. Malta and M. A. Aegerter, J.Alloys. Comp., 227 (1995) 135.
21. B.R. Judd, Phys Rev. B, 127 (1962) 750.
22. G.S. Ofelt, J. Chem. Phys, 37 (1962) 511.
23. Vineet Kumar Rai, S.B.Rai and D.K.Rai, Sensors and Actuators Physical-A, 128 (2006) 14
24. Garima Tripathi, Vineet Kumar Rai and S. B. Rai, Appl. Phys. B (Laser and Optics) 84(2006)459.
25. H. Kusuma, O.J. Sovers and T.Yoshika, Jap.J. Applied Physics 15 (1976) 2349